Tunneling in the Delayed Luminescence of Colloidal CdSe, Cu^+-Doped CdSe, and $CuInS_2$ Semiconductor Nanocrystals, and Relationship to Blinking

Arianna Marchioro,[‡] Patrick J. Whitham,[‡] Kathryn E. Knowles,[§] Troy B. Kilburn, Philip J. Reid, and Daniel R. Gamelin*

Department of Chemistry, University of Washington, Seattle, WA 98195-1700, USA

**Electronic address: gamelin@chem.washington.edu*

[‡]*These authors contributed equally*

Abstract. The photoluminescence decay dynamics of colloidal CdSe, Cu^+:CdSe, and $CuInS_2$ nanocrystals have been examined as a function of temperature and magnetic field. All three materials show photoluminescence decay on timescales significantly longer than the intrinsic lifetimes of their luminescent excited states, *i.e.*, delayed luminescence, involving formation of a metastable trapped excited state followed by detrapping to reform the emissive excited state. Surprisingly, the delayed luminescence decay kinetics are nearly identical for these three very different materials, suggesting they reflect universal properties of the delayed luminescence phenomenon in semiconductor nanocrystals. By measuring luminescence decay over 8 decades in time and 6 decades in intensity, we observe for the first time a clear deviation from power-law dynamics in delayed luminescence. Furthermore, for all three materials, the delayed luminescence decay dynamics are observed to be nearly independent of temperature between 20 K and room temperature, reflecting tunneling as the dominant mechanism for detrapping from the metastable state. A kinetic model is introduced that invokes a log-normal distribution of tunneling rates and reproduces the full range of delayed luminescence decay dynamics well. These findings are discussed in relation to photoluminescence blinking, with which delayed luminescence appears closely associated.

Introduction

Delayed luminescence, or the observation of photoluminescence (PL) on timescales much longer than the material's intrinsic luminescence lifetime, has recently been recognized as an integral and possibly universal feature of colloidal semiconductor nanocrystal photophysics, appearing in various CdSe,[1-5] Cu^+-doped CdSe (Cu^+:CdSe),[3] and ternary copper indium sulfide ($CuInS_2$)[6] nanocrystals (NCs) with and without additional shell layers. Delayed luminescence has been attributed to formation of a metastable charge-separated state, in which one or both of the charge carriers are trapped, followed by slow detrapping to repopulate the intrinsic emissive state. Delayed luminescence decay does not follow simple exponential kinetics, but instead displays distributed kinetics spanning from sub-microsecond to seconds.[1-6] Although the delayed luminescence amplitude is small relative to the total PL amplitude during photoexcitation (~1%),[6] delayed luminescence can account for a large fraction of the total emission after an excitation pulse (from ~10%[4,6] to as much as ~50%[5]). This reversible charge-carrier trapping is thus not necessarily detrimental to quantum yield (QY); indeed, QYs as large as 50% have been recorded in CdSe platelets for which ~50% of the emission following a short laser pulse comes from delayed luminescence.[5] Photoexcitation power-dependence measurements show facile saturation of the delayed luminescence intensities,[6] indicating that photoexcitation of NCs already in the metastable state is followed by efficient nonradiative decay. Elongation of the prompt PL decay time through either hole localization[3] or NC photonic cavity effects[4] increases the fraction of PL coming from delayed luminescence, indicating that the metastable state is populated directly from the relaxed emissive state. Comparisons between Cu^+-doped and undoped CdSe NCs suggest specifically that electron trapping and detrapping are the rate-determining steps in the delayed luminescence of these NCs.[3]

A link between delayed luminescence and single-NC PL blinking was proposed as early as 2008,[1] when similar power-law coefficients were observed in sub-microsecond delayed luminescence and blinking data collected on a timescale of seconds for the same CdSe-based single NCs.[1,7] The “on”- and “off”-state statistics from PL blinking measurements generally display distributed kinetics and are most commonly fitted using power-law functions.[8,9] Several models have been proposed to explain these dynamics,[10-15] most of which invoke charge-carrier localization in the "off" state.[16,17] To account for the large integrated delayed luminescence intensities following short excitation pulses, it has been proposed that blinking "on" periods are

characterized by rapid carrier trapping and detrapping that cycles faster than successive photoexcitation events.[4]

Although many complementary approaches have been applied to characterize NC blinking, delayed luminescence has not yet been thoroughly explored, and a great deal remains to be learned from such measurements. Here, we describe new observations pertaining to the delayed luminescence of CdSe, Cu^+:CdSe, and $CuInS_2$ NCs. Despite their very different chemical compositions and spectroscopic characteristics, all three materials show remarkably similar delayed luminescence, but with key differences related to their different electronic structures. In particular, all three samples show delayed luminescence dynamics that are nearly temperature independent from 20 K to room temperature. This observation indicates a similar tunneling mechanism for detrapping from the metastable states of all three materials. Moreover, in all three materials, the delayed luminescence decay clearly deviates from power-law behavior, a characteristic that has not been noted previously. A tunneling model is introduced showing that these dynamics can be accounted for by invoking a Gaussian distribution of tunnel barriers, which results in a log-normal distribution in tunneling (detrapping) rates. The implications of these results and analysis are discussed and related to existing blinking models.

Experimental

Synthesis of $CuInS_2$ Nanocrystals. $CuInS_2$ NCs were synthesized by a method adapted from the literature.[18] A mixture of indium acetate (0.292 g, 1 mmol), copper iodide (0.190 g, 1 mmol), and dodecanethiol (5 mL) in a 50 mL three-neck round-bottom flask was degassed with three pump-purge cycles using nitrogen at room temperature. The reaction mixture was heated to 110 °C under nitrogen and held for 10 minutes until the solution turned optically clear and pale yellow. The reaction mixture was then heated to 230 °C. The solution turned dark orange at ~ 220 °C, and was very dark red by 230 °C. The reaction was held for 10 min. at 230 °C, after which the vessel was cooled rapidly to <60 °C. NCs were purified with several cycles of precipitation with ethanol and centrifugation followed by resuspension in toluene. Powder X-ray diffraction of the $CuInS_2$ NCs shows they have the chalcopyrite crystal phase (see Supporting Information).

Synthesis of CdSe and Cu^+:CdSe Nanocrystals. CdSe and Cu^+:CdSe NCs were synthesized by a heat-up method adapted from recent literature.[19] Briefly, $Cd(oleate)_2$ was synthesized *via*

adaptation of a cadmium myristate synthesis in the above reference. Sodium hydroxide (0.40 g, 10 mmol) and oleic acid (2.82 g, 10 mmol) were dissolved in 100 mL of methanol at 60 °C in ambient atmosphere. Cadmium nitrate tetrahydrate (6.16 g, 20 mmol) was dissolved in 16 mL methanol and added dropwise to the sodium oleate solution at 60 °C in ambient atmosphere under vigorous stirring. After addition, the reaction mixture was stored in a freezer overnight and then washed with cold methanol ~5 times. The solid product was collected by filtration and dried under vacuum. The final product is a white powder, and is stored under inert atmosphere to slow oxidation. 0.2025 g of the prepared Cd(oleate) solution, 0.0334 g SeO_2 and 13.22 g ODE were degassed at 55 °C with three pump-purge cycles with N_2 in a separate reaction flask. The reaction mixture was heated to 235 °C under N_2. The mixture turned pale yellow at ~180 °C and was pale orange when the reaction reached 235 °C, after 5 min the solution was dark red. At this point a 5 mL aliquot of CdSe NCs was removed.

In a separate reaction flask, 0.019 g CuCl and 2.40 g octadecene were degassed by bubbling with N_2. Then 0.1 mL tri-octylphosphine was added to the CuCl mixture. 1.5 mL of the CuCl mixture was injected into the CdSe NC reaction flask. 1 mL aliquots were removed from the Cu^+:CdSe NC reaction at 10, 20, and 25 min following injection. The remaining 1.5 mL of CuCl solution was injected after the 25 min aliquot, additional aliquots were taken 10 and 15 min after the second injection. Finally, 20 min after the second injection, the remaining reaction mixture was cooled to room temperature. The CdSe aliquot and final Cu^+:CdSe reaction mixtures were then purified by precipitation with ethanol and centrifugation, the NC pellet was washed with acetone followed by NC resuspension in toluene.

General Characterization. Samples were characterized by UV-Vis absorption spectroscopy, transmission electron microscopy, and ensemble photoluminescence. Cu^+:CdSe was also characterized by inductively coupled plasma atomic emission spectroscopy (ICP-AES), and $CuInS_2$ by powder X-ray diffraction (see Supporting Information (SI)).

Spectroscopic Characterization. Absorption spectra of CdSe, Cu^+:CdSe, and $CuInS_2$ NCs suspended in toluene were measured using a Varian Cary 5000 spectrometer. Solution-phase PL spectra were measured using an Ocean Optics USB-2000+ spectrometer with 405 nm excitation. PL spectra were corrected for the instrument response unless otherwise indicated.

Temperature-dependent Photoluminescence Lifetimes. Temperature-dependent PL decay measurements were performed on drop-coated films of NCs sandwiched between quartz disks

and mounted in a closed-cycle helium cryostat. Samples were excited using a 405 nm diode laser modulated with a square pulse waveform output from a function generator (SRS, DS345). Excitation pulse durations were kept constant at 50 ms and cycle periods were varied from 55 ms to 3.3 s depending on the time window of interest. PL decay traces were measured near the peak emission maximum for each sample with a bandwidth of < 20 nm. The PL was passed through a 420 nm long-pass filter and focused into a monochromator (0.5 m, 150 g/mm grating blazed at 500 nm) equipped with a PMT. Decay traces were collected over multiple time windows from 10 μs to 2.6 s. The signal was processed using a multichannel scaler and collected with a custom LabView program. Temperatures were varied from 20 K to 295 K.

Magnetic Circularly Polarized Luminescence. For magnetic circularly polarized luminescence (MCPL) measurements, drop-coated films of NCs sandwiched between quartz disks were loaded into a superconducting magneto-optical cryostat with a variable-temperature sample compartment (Cryo-Industries SMC-1659 OVT). A 405 nm diode laser was used for photoexcitation at an incident angle of ~20° relative to the optical detection axis. Excitation was modulated at 500 Hz with the square wave output from a function generator. PL was collected along the magnetic field axis (Faraday geometry), passed through a liquid crystal variable retardation plate set to $\lambda/4$ at the emission maximum, followed by a linear polarizer used to separate left and right circularly polarized PL components. A 420 nm long-pass filter placed after the linear polarizer removed scattered excitation light before the PL was collected by an optical fiber and directed into a monochromator. Spectra were collected with a LN_2 cooled CCD. PL lifetimes were collected with a PMT connected to a multichannel scaler. PL was measured at constant wavelengths, 760 nm for Cu^+:CdSe and 740 nm for $CuInS_2$, with bandwidths ~10 nm. MCPL polarization ratios were calculated from the relative intensities of left and right circularly polarized PL at various applied magnetic field strengths, following the sign convention described in Piepho and Schatz.[20]

Time-Resolved Photoluminescence Spectra. Temperature-dependent PL measurements were performed on films of NCs sandwiched between quartz plates. The films were measured in a flow cryostat cooled at liquid helium temperature. A 405 nm diode laser (2 mW, 4 mm spot) was used for photoexcitation at an incident angle of ~90° relative to the optical detection axis. Excitation was modulated at 100 Hz for Cu^+:CdSe and $CuInS_2$ NCs and at 5000 Hz for CdSe NCs, with a square pulse waveform output from a function generator (SRS, DS345). TRPL data

containing both the ON and OFF pulse periods were recorded using a streak camera (Hamamatsu, C10627) combined with a monochromator and synchronized with the square-wave generator.

Results and Analysis

Absorption and Photoluminescence Spectra. Figure 1 summarizes the absorption and PL spectra of the colloidal CdSe, Cu^+:CdSe, and $CuInS_2$ NCs investigated here. Unless otherwise noted, these samples were used for all subsequent experiments, but very similar results are obtained for other samples of the same materials. Figure 1A shows absorption and PL spectra of CdSe NCs suspended in toluene. The first excitonic absorption feature is centered at 2.25 eV. A sharp excitonic PL band is observed centered at 2.19 eV, with a small and broad trap PL feature observable centered at ~1.5 eV. The PL of the Cu^+:CdSe NCs shown in Figure 1B is dominated by a broad PL band centered at 1.38 eV associated with recombination of a delocalized conduction-band electron and a copper-localized hole.[21] A small amount of residual excitonic PL is observed at 2.12 eV, attributable to the presence of some undoped CdSe NCs within the NC ensemble. Figure 1C shows the absorption and PL spectra of $CuInS_2$ NCs. This PL spectrum consists of a broad band centered at 1.7 eV, commonly associated with recombination involving one or more deeply trapped carriers.[21] TEM images are provided for each sample, showing pseudo-spherical NCs in each case.

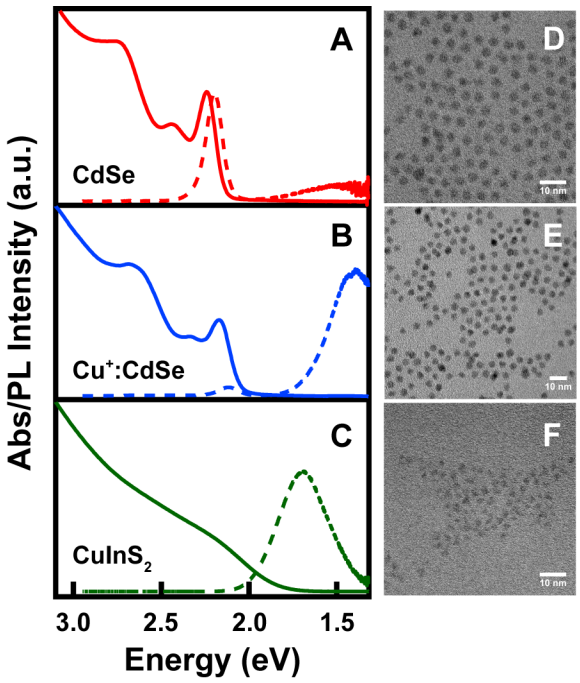

Figure 1. Room-temperature electronic absorption and photoluminescence spectra of **(A)** CdSe, **(B)** Cu^+:CdSe (~0.7 % copper), and **(C)** $CuInS_2$ NCs suspended in toluene. TEM images of these **(D)** CdSe, **(E)** Cu^+:CdSe, and **(F)** $CuInS_2$ NCs. The scale bars represent 10 nm. The diameters of 100 NCs were measured for each sample, yielding mean values of (D) 4.3 ± 0.4 nm, (E) 5.1 ± 0.5 nm, and (F) 3.9 ± 0.7 nm, respectively.

Luminescence Decay. Figure 2 plots 20 K PL decay traces for the same undoped CdSe, Cu^+:CdSe, and $CuInS_2$ NCs of Figure 1 using a double-log representation. All three traces show distributed decay kinetics spanning many orders of magnitude in time. Two clearly separable time regimes can be identified. The first regime corresponds to prompt decay of the luminescent excited state and accounts for the majority of the luminescence amplitude. Fitting this prompt luminescence to a single exponential in each case yields lifetimes of *ca*. 40 ns (CdSe), 1 μs (Cu^+:CdSe), and 2 μs ($CuInS_2$). The second regime consists of PL decay that persists long after the prompt decay is complete. This component is referred to as delayed luminescence. The CdSe NCs exhibit substantially less delayed luminescence than displayed by either the Cu^+:CdSe or $CuInS_2$ NCs under otherwise essentially identical conditions. We interpret this difference as indicating that the shorter lifetime of the CdSe NC emitting state allows less time for trapping into the metastable state.[3] Note that this interpretation requires different trapping and detrapping rates, which could conceivably arise from a dynamic dispersion mechanism, but the present data

do not specifically probe trapping dynamics so further interpretation would be speculative.

Surprisingly, all three materials show remarkably similar dispersed kinetics in their delayed luminescence decay, extending over several orders of magnitude in time. In each case, these kinetics show a distinct deviation from power-law behavior, which would be linear in the double-log representation of Figure 2. We suggest that the observation of nearly parallel delayed luminescence decay curves for three very different types of NCs (CdSe, Cu^+:CdSe, and $CuInS_2$) argues that this curvature is a property of the detrapping phenomenon itself and does not originate from power-law truncation *via* a completely independent process like non-radiative decay, because the latter would likely be strongly sample dependent. Intrinsic deviation of delayed luminescence decay from power-law dynamics has not been reported previously for any sample, but has important mechanistic implications.

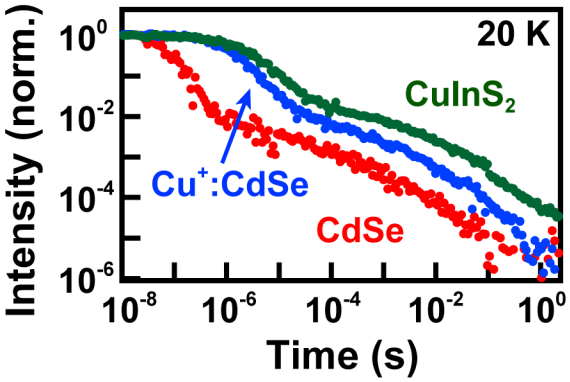

Figure 2. Double-log plot of 20 K PL intensity decay for $CuInS_2$, Cu^+:CdSe, and CdSe NCs, showing prompt and delayed luminescence regimes at short and long times, respectively. The CdSe NCs exhibit faster prompt decay and less delayed luminescence than either the $CuInS_2$ or Cu^+:CdSe NCs. The delayed luminescence for all three materials decays with remarkably similar dispersed kinetics extending over several orders of magnitude in time. The same data plotted on linear axes are presented in the Supporting Information.

Prompt and Delayed Luminescence Spectra and Magneto-Luminescence. Figure 3 plots PL spectra of the Cu^+:CdSe and $CuInS_2$ NCs measured during photoexcitation (prompt luminescence) and integrated between 25 μs and 1.2 ms after the end of the excitation pulse (delayed luminescence), when all prompt luminescence has decayed. The delayed luminescence spectra are very similar to the prompt luminescence spectra, consistent with the hypothesis that the emitted photons come from the same excited state in both prompt and delayed time regimes. We note that both samples show a small (< 40 meV) red shift of the delayed luminescence

relative to the prompt luminescence. Such a shift could conceivably be due to donor-acceptor pair recombination in the $CuInS_2$ NCs,[22,23] but this explanation is considered unlikely here because both samples in Figure 3 show essentially the same red shift even though the Cu^+:CdSe NCs decay *via* a free-to-bound ($ML_{CB}CT$) recombination mechanism.[21] Instead, this small redshift in both samples more likely arises from particle size inhomogeneity, in which smaller NCs show higher-energy emission, shorter prompt decay times,[24] and slightly less delayed luminescence (see below). Overall, these data support the interpretation that delayed luminescence involves slow detrapping to reform the intrinsic emissive excited state, rather than carrier recombination directly from the metastable state.

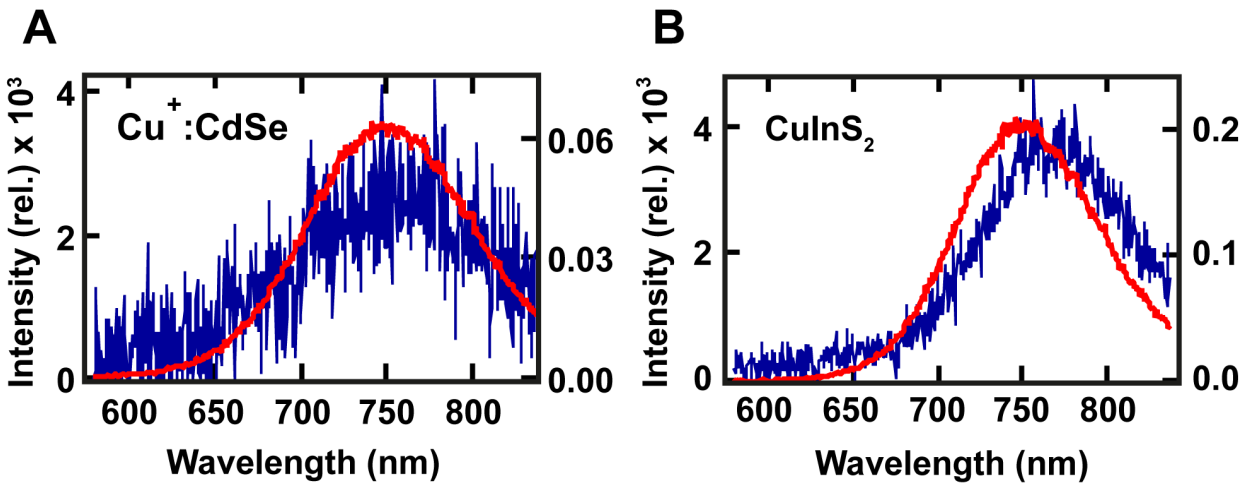

Figure 3. Prompt (red) and delayed (blue) photoluminescence spectra of **(A)** Cu^+:CdSe NCs and **(B)** $CuInS_2$ NCs, collected at 5 K. Spectra were not corrected for the instrument response. A constant baseline was subtracted from each delayed luminescence spectrum. The Cu^+:CdSe NCs are from a different synthetic batch but are spectroscopically nearly identical to those shown in Figures 1, 2, and 5 (see SI).

To test this interpretation in a more discriminating experiment, time-resolved magneto-PL measurements were performed. As reported previously,[25] Cu^+:CdSe and $CuInS_2$ NCs both display singlet-triplet excited-state exchange splittings, with the low-temperature luminescence originating from the lower-energy triplet state. Application of a magnetic field induces a Zeeman splitting of this triplet state, and at low temperatures the emission becomes partially circularly polarized. As the temperature is raised, the higher-energy singlet state is populated, but this singlet state is not split in a magnetic field and thus does not contribute to the magnetic circularly

polarized photoluminescence (MCPL) signal in first order. Consequently, the prompt MCPL intensities of Cu^+:CdSe and $CuInS_2$ NCs both decrease with increasing temperature in a characteristic temperature range defined by their singlet-triplet splitting energies. Here, we show that the delayed luminescence from these two materials shows the same MCPL and temperature dependence as their prompt luminescence.

Figures 4A,B show MCPL spectra of Cu^+:CdSe and $CuInS_2$ NCs collected at 1.6 K and 6 T. The intensity of right (σ^+) circularly polarized luminescence has increased and that of left (σ^-) circularly polarized luminescence has decreased in response to the magnetic field. These MCPL signals are quantified using the polarization ratio ($\Delta I/I$), defined as shown in eq 1.

$$\frac{\Delta I}{I} = \frac{\sigma^- - \sigma^+}{\sigma^- + \sigma^+} \qquad (1)$$

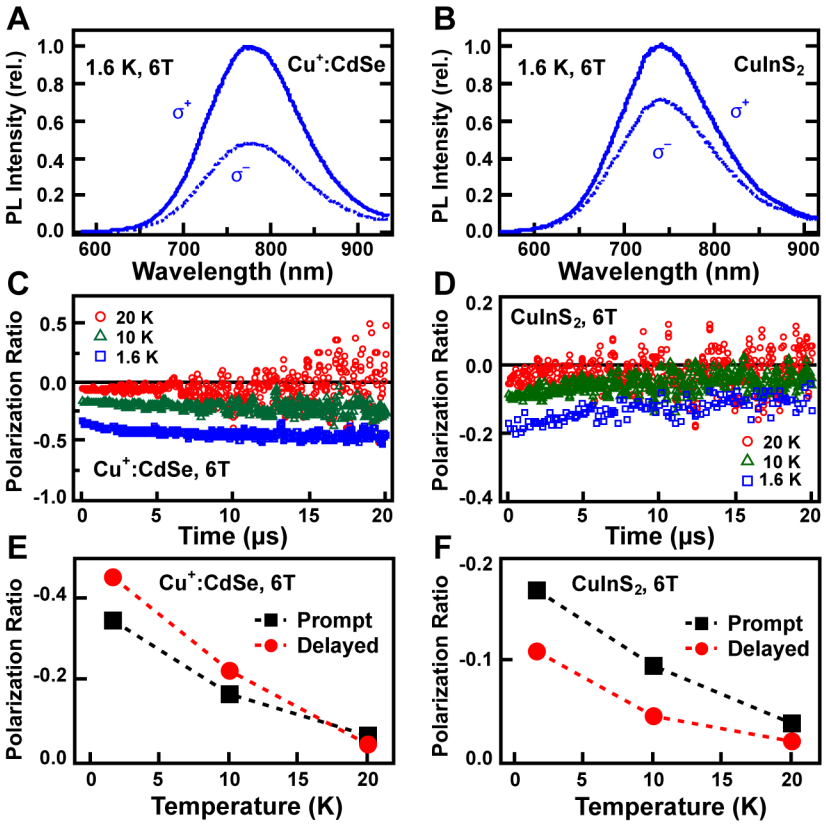

Figure 4. Magnetic circularly polarized photoluminescence (MCPL) spectra of **(A)** Cu^+:CdSe and **(B)** $CuInS_2$ NCs measured at 1.6 K, with an applied magnetic field of 6 T. Solid line: right circularly polarized, σ^+. Dashed line: left circularly polarized, σ^-. **(C,D)** MCPL polarization ratio ($\Delta I/I$) plotted *vs* luminescence decay time measured at 1.6 K (blue squares), 10 K (green triangles), and 20 K (red circles) for (C) Cu^+:CdSe and (D)

$CuInS_2$ nanocrystals, all at 6 T. $\Delta I/I$ is measured at the prompt luminescence maximum. **(E,F)** $\Delta I/I$ plotted *vs* temperature for prompt (black) and delayed (red) luminescence. The delayed luminescence values represent $\Delta I/I$ averaged between 10 and 20 μs after the end of the excitation pulse, well after the decay of the prompt luminescence. The Cu^+:CdSe NCs are from the same sample as in Figure 3 (see SI).

Figures 4C,D plot $\Delta I/I$ measured from 0 to 20 μs following the end of a photoexcitation pulse for the same Cu^+:CdSe and $CuInS_2$ NC samples, measured at 6 T and three different temperatures (1.6, 10, and 20 K). The full decay traces for σ^+ and σ^- polarized light are provided as Supporting Information. Similar behavior is observed for both samples. To our knowledge, transient MCPL data have not been reported for these materials previously. In accordance with our previous steady-state measurements,[25] the magnitude of $\Delta I/I$ is greatest at the lowest temperature and decreases with increasing temperature at all measurement times, with the same signs and similar values of $\Delta I/I$ observed in both the prompt and delayed luminescence regimes at each temperature. We note that for both samples, $\Delta I/I$ does change slightly during the full PL decay period. These changes are consistent with the small red-shift in PL energy, and are again attributed to NC inhomogeneity. Figures 4E,F summarize these data, plotting $\Delta I/I$ for the prompt and delayed luminescence components *vs* temperature for these two samples. Both prompt and delayed MCPL show very similar values of $\Delta I/I$ and identical trends with temperature, consistent with the delayed luminescence originating from the same electronic state that gives rise to the prompt luminescence in each sample. In particular, these results conclusively eliminate the possibility that delayed luminescence in either sample comes from donor-acceptor-pair recombination directly from the metastable charge-separated state: To achieve such long recombination times, this charge-separated state must have a substantially smaller electron-hole exchange coupling strength than the prompt emissive state, and hence should show substantially smaller MCPL and a significantly different MCPL temperature dependence from that observed in the prompt luminescence.

Temperature Dependence of Delayed Luminescence. Figure 5 summarizes the temperature dependence of the CdSe, Cu^+:CdSe, and $CuInS_2$ NC PL dynamics. Figures 5A-C plot PL decay curves for each sample, measured at various temperatures between 20 K and room temperature and from nanoseconds to seconds. The PL decay curves of the CdSe NCs (Figure 5A) are essentially temperature independent between 20 K and room temperature, showing only a small

and gradual drop in both the prompt and delayed luminescence intensities with increasing temperature. The Cu^+:CdSe and $CuInS_2$ NCs show a stronger temperature dependence. With increasing temperature, the amplitude of the prompt luminescence of the Cu^+:CdSe NCs (Figure 5B) changes little but the delayed luminescence amplitude appears to decrease substantially, even though the long-time dynamics remain nearly parallel at all temperatures. This trend is even more pronounced in the data from the $CuInS_2$ NCs (Figure 5C). For this sample, the delayed luminescence intensity appears anomalously low at room temperature, attributed to the onset of a new thermally activated nonradiative decay channel.

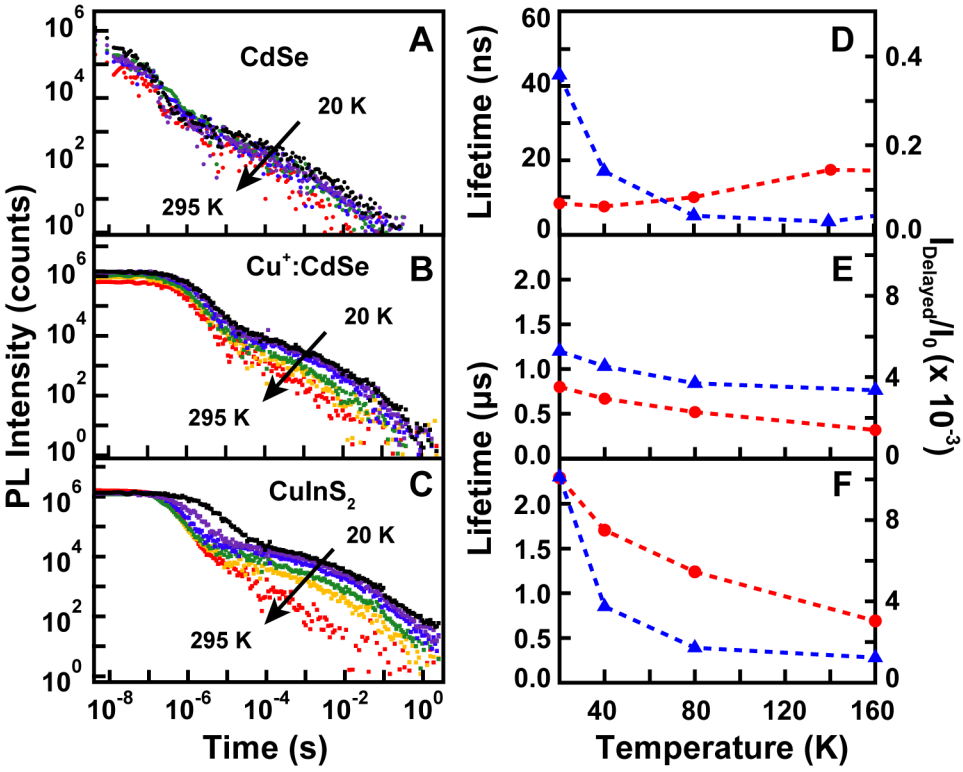

Figure 5. (A, B, C) Double-log plots of PL intensity decay for (A) CdSe, (B) Cu^+:CdSe NCs, and (C) $CuInS_2$ NCs collected from 20 to 295 K. Color code: black = 20 K, purple = 40 K, green = 80 K, blue = 140 K (CdSe) or 160 K (Cu^+:CdSe & $CuInS_2$), yellow = 200 K, red = 295 K. The same data plotted on linear axes are presented in the Supporting Information. **(D, E, F)** Temperature dependence of prompt luminescence decay lifetimes from single-exponential fits (τ_{prompt}, blue triangles,) and the ratio of delayed to steady-state luminescence intensities ($I_{delayed}/I_0$, red circles), where I_0 is the steady-state luminescence intensity measured during photoexcitation and $I_{delayed}$ is the luminescence intensity measured 450 μs after termination of the photoexcitation. (D) CdSe NCs, (E) Cu^+:CdSe NCs, and (F) $CuInS_2$ NCs.

Accurately integrating the total delayed luminescence during decay is difficult because of overlap between prompt and delayed intensities at short times, where the prompt luminescence dominates. This overlap requires extrapolation of the weak delayed luminescence decay curve over precisely the time window where its amplitude is greatest, introducing substantial uncertainty. With this limitation in mind, we estimate that delayed luminescence accounts for at least ~70% ($CuInS_2$), ~50% (Cu^+:CdSe), and ~30% (CdSe) of all photons emitted after termination of the excitation pulse in the 20 K data of Figure 5A-C, but we stress that these estimates can vary greatly depending on the extrapolation method used. Moreover, as demonstrated previously, the delayed luminescence intensity is strongly dependent upon experimental conditions, including excitation power.[6] Photoexcitation of NCs already in a metastable charge-separated state results in nonradiative Auger relaxation, and the long lifetimes of these states can thus be expected to influence luminescence quantum yields measured under some cw excitation conditions. Although the specific numbers may not be significant in any absolute sense, it is clear that delayed luminescence can constitute a very large fraction of the total emission following an excitation pulse.

A more reliable way to quantify the relative delayed luminescence amplitude is by analyzing $I_{delayed}/I_0$, which represents the ratio of the delayed PL intensity ($I_{delayed}$, measured 450 μs after termination of illumination, where no prompt PL occurs) to the steady-state PL intensity (I_0, measured under cw illumination). Because the delayed luminescence decay kinetics are largely independent of temperature (Figure 5 and SI), $I_{delayed}$ is approximately proportional to the total delayed luminescence amplitude. Likewise, the small steady-state amplitude of the delayed luminescence means that I_0 is very nearly equivalent to the prompt luminescence amplitude.[6] Figures 5D-F plot $I_{delayed}/I_0$ *vs* temperature for the CdSe, Cu^+:CdSe, and $CuInS_2$ NCs, respectively, all with absolute *y*-axis scaling. From these plots, it is evident that $I_{delayed}/I_0$ is an order of magnitude larger for the two copper-containing NCs than it is for the CdSe NCs. For the Cu^+:CdSe and $CuInS_2$ NCs, $I_{delayed}/I_0$ decreases with increasing temperature, whereas for the CdSe NCs $I_{delayed}/I_0$ shows a much smaller but more complicated temperature dependence. Specifically, the CdSe NC data are complicated by the presence of deep-trap luminescence (*e.g.*, Figure 1A). Both exciton and deep-trap delayed luminescence are observed from these CdSe NCs, but the trap luminescence carries much more relative intensity during delayed luminescence than under cw excitation (see SI), similar to data reported for CdSe and CdSe/CdS

nanoplatelets.[5] These data demonstrate the existence of (at least) two qualitatively different types of trap states in CdSe NCs: (*i*) non-emissive metastable trap states that are essentially degenerate with the lowest excitonic states and that decay by detrapping to reform excitons, and (*ii*) deep trap states that can decay by emission of mid-gap photons. From comparison of CdSe and Cu^+:CdSe NCs, we have previously argued that the former involves reversible electron trapping.[3] The relative increase in CdSe NC mid-gap luminescence during delayed luminescence suggests that this deep trapping becomes more likely after the excited NC enters the metastable state, consistent with the emissive mid-gap trap state involving deep hole trapping. Understanding the relationship between this emissive mid-gap trap state and the non-emissive metastable state in CdSe and related NCs poses an interesting challenge for future studies that can perhaps be addressed *via* additional delayed luminescence measurements.

Figures 5D-F also plot the prompt luminescence lifetime (τ_{prompt}) *vs* temperature for the same three samples. The data for the Cu^+:CdSe and $CuInS_2$ NCs, which are not complicated by the competing deep-trap luminescence seen in the CdSe NCs, demonstrate a strong positive correlation between τ_{prompt} and $I_{delayed}/I_0$. The variations in $I_{delayed}/I_0$ are thus interpreted as reflecting variations in τ_{prompt} because the probability of populating the metastable state responsible for the delayed luminescence is proportional to the lifetime of the emissive excited state that feeds this metastable state. The smaller $I_{delayed}/I_0$ of the CdSe NCs is consistent with their shorter τ_{prompt}, bearing in mind the caveat of additional hole trapping discussed above.

Kinetic Model. Three important observations arise from the delayed luminescence dynamics ($t > \sim 10^{-4}$ s) shown in Figure 5: (*i*) The delayed luminescence decay is highly non-exponential, requiring a distribution of rate constants to account for these dynamics, (*ii*) log-log plots of the delayed luminescence decay data for all three samples show significant curvature, indicating that the underlying distributions of rate constants cannot be described by the power-law expressions used to date,[1,4,5] and (*iii*) the dynamics of delayed luminescence are temperature independent, which implies that the rate-limiting detrapping step involves tunneling. Similar temperature-independent delayed luminescence has recently been reported for CdSe nanoplatelets over a shorter time window,[5] supporting the generality of this observation. Here, we demonstrate that all three of these key features can be accounted for simultaneously in a single kinetic model by invoking a log-normal distribution of tunneling rate constants.

The kinetic model used to describe the variable-temperature PL decay dynamics shown in Figure 5 combines prompt PL with a continuous distribution of tunneling rate constants governing the delayed luminescence decay (eq 2).

$$I(t) = A_P \exp(-k_{prompt} t) + A_D \int_0^\infty p(a) \cdot \exp(-k_{tunnel}(a) \cdot t)\, da \qquad (2)$$

The first term in eq 2 describes the prompt luminescence decay and the second describes the delayed luminescence. The parameters A_P and A_D represent the amplitudes of prompt and delayed luminescence, respectively. $k_{prompt} = 1/\tau_{prompt}$ describes the prompt luminescence decay rate constant, as summarized in Figure 5. The tunneling rate constant, k_{tunnel}, depends exponentially on the tunneling barrier width a, as described by eq 3, where β is the tunneling decay constant.

$$k_{tunnel}(a) = k_0 \exp(-\beta a) \qquad (3)$$

The term $p(a)$ in eq 2 represents the distribution of tunnel widths. Here, we model $p(a)$ as a Gaussian distribution using eq 4.

$$p(a) = \frac{1}{\sigma\sqrt{2\pi}} \exp\left(\frac{-(a - \langle a \rangle)^2}{2\sigma^2}\right) \qquad (4)$$

In eq 4, $\langle a \rangle$ is the average tunnel width and σ is the standard deviation defining the Gaussian distribution. Eq 4 can be rewritten in terms of k_{tunnel} to give:

$$p(k_{tunnel}(a)) = \frac{1}{\sigma\sqrt{2\pi}} \exp\left(\frac{-(\ln(k_{tunnel}(a)) - \langle \ln(k_{tunnel}(a)) \rangle)^2}{2(\beta\sigma)^2}\right) \qquad (5)$$

Eq 5 illustrates that the tunneling rate constants emerging from a Gaussian distribution of tunnel barriers are log-normally distributed.

This model captures the key features of the experimental data remarkably well. Figure 6 plots the results of this model in comparison with the experimental data from the Cu^+:CdSe NCs. These data were chosen as representative of all three data sets in Figure 5 and are used here because they have better signal-to-noise ratios than the CdSe NC data and they show less nonradiative decay than the $CuInS_2$ NC data at room temperature. For modeling this data set, the prompt luminescence decay was fit at each temperature, and a single set of parameters was used to describe the delayed luminescence at all temperatures, with the exception of A_D, which is temperature dependent as reflected in the data of Figure 5E (note that $A_D/(A_P + A_D) \propto I_{delayed}/I_0$). The good agreement between the simulated and experimental delayed luminescence data

summarized in Figure 6 implies that the rate constants for delayed luminescence follow a temperature-independent log-normal distribution with $k_{tunnel}(\langle a \rangle) \approx 5 \times 10^4$ s^{-1}. The full distribution in k_{tunnel} is derived from a $\sigma = 30\%$ standard deviation about the mean tunnel-barrier width, $\langle a \rangle$, with $\beta\langle a \rangle >> 1$. Rate constants smaller than 10^3 s^{-1} account for ~10% of the delayed luminescence intensity. The prominence of such small rate constants is responsible for the remarkable observation of luminescence even seconds after photoexcitation. Interestingly, the average tunneling rate constant has a value of $\langle k_{tunnel}(a) \rangle \approx 4.1 \times 10^6$ s^{-1}, consistent with a significant fraction of trapping/detrapping actually occurring on the same timescale as prompt luminescence in this sample, as evident from visual inspection of Figure 6. The very similar delayed luminescence observed in all three data sets of Figure 5 indicates that the same log-normal distribution can be applied for all three NC samples investigated here, with different specific parameters to account for their different prompt luminescence dynamics and nonradiative decay at elevated temperatures.

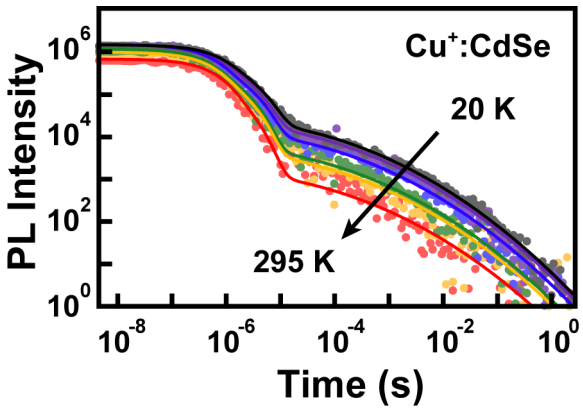

Figure 6. Simulated luminescence decay curves reproducing the Cu$^+$:CdSe NC data from Figure 5, calculated using eq 2. The first 160 μs of the prompt luminescence decay at each temperature was fitted to a sum of two exponentials, summarized by the average lifetime data shown in Figure 5E. The delayed luminescence was modeled as a tunneling process using $k_0 = 10^9$ s^{-1} and a Gaussian distribution in tunneling barrier widths defined by $\langle a \rangle = 1.0$ and $\sigma = 0.3$, with a tunnel decay constant of $\beta = 10$ (all given in reduced units). The same parameters were used for simulation of the delayed luminescence at all temperatures, with the exception of A_D, which is temperature dependent. See main text and SI for additional details.

We note that although this model reproduces the salient features of the experimental data very well, the simulated curves in Figure 6 do not represent optimized fits of the data. Given the number of unknown variables in the model, we are unable to identify a unique set of best-fit parameters by least-squares procedures. For this reason, we do not analyze the specific model parameters further. Instead, we highlight the new general conclusions that can be drawn from this analysis, namely that a non-power-law distribution of tunneling rates is required to describe the delayed luminescence decay dynamics, and that the key features of this decay are reproduced well using a temperature-independent log-normal distribution of tunneling rates, as would arise from a tunneling process involving a Gaussian distribution of tunnel-barrier widths.

Discussion

The data presented here reveal surprisingly similar delayed luminescence phenomena in three qualitatively distinct types of colloidal semiconductor NCs, CdSe, Cu^+:CdSe, and $CuInS_2$. From these results, we hypothesize that delayed luminescence is a universal feature of the photophysics of colloidal chalcogenide-based semiconductor nanocrystals, and is likely even more general among colloidal semiconductor nanocrystals. In each of the materials investigated here, delayed luminescence decay shows distributed kinetics that are not describable by a power law over the full 8 orders of magnitude in experimentally measured decay time. Such non-power-law dynamics are not evident from previous reports of NC delayed luminescence, presumably because data were not collected over sufficiently long time windows. Strikingly, for all three nanocrystal types examined here, the delayed luminescence kinetics are temperature independent between 20 K and at least 160 K. This distinctive temperature independence provides strong evidence that delayed luminescence involves detrapping from a metastable excited state *via* a tunneling mechanism as a general feature in various types of semiconductor NCs. At temperatures approaching room temperature, a thermally activated nonradiative decay channel emerges that appears to be material (and likely sample) dependent.

Figure 7 uses a single-configurational-coordinate diagram to illustrate schematically the process of carrier detrapping *via* tunneling implied by the data presented here. Analysis shows that the distributed decay kinetics displayed by the delayed luminescence are reproduced well over all 8 orders of magnitude in time when using a temperature-independent Gaussian distribution in tunnel widths ($\sigma = 30\%$), corresponding to a log-normal distribution in tunneling

rates. Such a distribution in tunnel widths could conceivably arise from a distribution in the displacement of the metastable state's potential energy surface relative to the emissive state's surface along the tunneling coordinate, or could arise from a distribution in tunneling driving forces; our data do not speak to the microscopic origin of the distribution. In either scenario, such distributions are assumed to be generated by local chemical variations at the NC surfaces, such as inhomogeneous ligand, ion, or surface-dipole distributions.

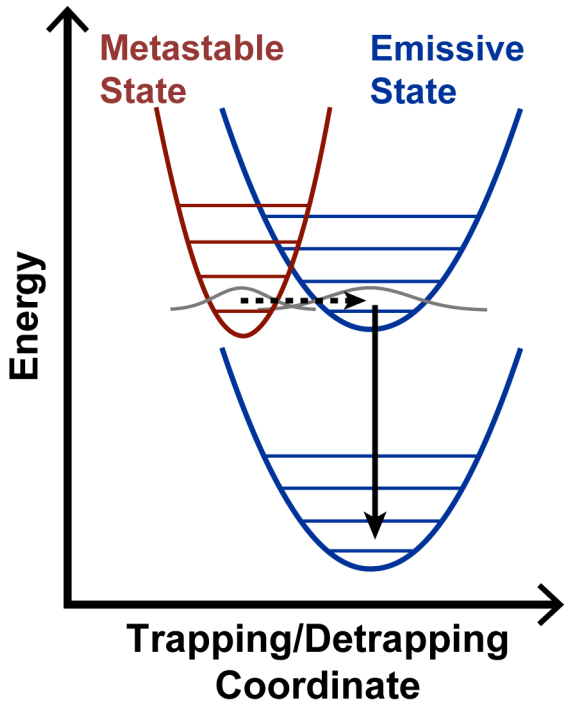

Figure 7. Single-configurational-coordinate diagram illustrating the generation of delayed luminescence by detrapping from a metastable charge-separated excited state. Detrapping occurs by tunneling from this metastable state to the emissive state (dashed arrow). Delayed luminescence is observed upon subsequent radiative decay to the ground state (solid arrow). The experimental decay dynamics indicate a Gaussian distribution in tunnel-barrier widths, corresponding to a log-normal distribution in tunneling rates.

Despite the temperature independence of the delayed luminescence kinetics, the delayed luminescence amplitude can change with temperature for a given sample. We propose that this observation reflects the temperature dependence of the prompt luminescence decay times and illustrates the competition within the emissive excited state between prompt luminescence and formation of the metastable state. For the same reason, materials with much longer prompt

luminescence lifetimes (Cu^+:CdSe and $CuInS_2$ NCs, compared to CdSe NCs) show much greater delayed luminescence amplitudes relative to their prompt luminescence ($A_D/(A_P + A_D)$, or $I_{delayed}/I_0$).[3] In CdSe NCs, an additional competition exists involving formation of a luminescent deep-trap state. The observation that delayed luminescence intensities are influenced by changes in prompt luminescence lifetimes from 10 ns to 10 μs illustrates that trapping into the metastable state must occur over at least 4 orders of magnitude in time. This finding is consistent with our previous conclusion of distributed trapping dynamics, inferred from the excitation-power dependence of room-temperature delayed luminescence intensities in $CuInS_2$ NCs.[6] Moreover, although trapping is primarily restricted to ns - μs timescales by the prompt luminescence lifetime, detrapping can occur on much longer timescales (≥ sec). This asymmetry would not be expected from a static tunneling scenario, and we suggest that it reflects important dynamical fluctuations of the metastable state relative to the emissive excited state.

We note in passing that the similarity in delayed luminescence decay dynamics among these three very different NCs should not be construed as necessarily implying similar microscopic identities of their traps. Instead, this similarity is likely due in large part to the fact that the phenomenon itself is strongly biased toward the scenario of nearly degenerate emissive and metastable trapped excited states;[2] A trapped excited state too far above the emissive excited state is unlikely to form and unlikely to detrap slowly, while a trapped excited state too far below the emissive state may likely form but is unlikely to detrap to yield a delayed emission event.

As discussed in the Introduction, there is growing evidence of a mechanistic link between delayed luminescence and photoluminescence blinking in colloidal semiconductor nanocrystals.[1,3-6] The data and analysis presented here bolster proposals of such a link. Although power-law behavior is often reported in blinking studies[8,9,26] and has been reported for delayed luminescence as well,[1,4,5] deviations from power-law have been emphasized in recent blinking literature.[27-29] Deviations from power-law kinetics are clearly evident in the delayed luminescence kinetics reported here. For both delayed luminescence (this study) and some blinking data,[27-29] log-normal distributions reproduce the dynamics better than power-law distributions. Even more compelling is the observation in blinking measurements on CdSe NCs that the "off" statistics (which reflect detrapping dynamics analogous to the delayed luminescence decay dynamics described here) are also temperature independent,[8,9,26,30,31] implying a tunneling process for detrapping. The tunneling process illustrated in Figure 7 is thus

directly analogous to the tunneling mechanism of carrier detrapping invoked in several PL blinking models.[8,10,11] As stressed previously,[8] a ~25% variation in the mean trap distance can generate a 10^7-fold variation in tunneling times, and hence could account for the broadly distributed blinking "off" dynamics. Here, we find that a 30% variation in the mean tunnel width reproduces the distributed delayed luminescence dynamics well (Figure 6). Whereas stochastic trap-state fluctuations must be explicitly invoked to account for single-particle blinking dynamics,[8,11,14,26] ensemble delayed luminescence measurements integrate over all such fluctuations within the ensemble, allowing adequate description of the dynamics using a static distribution of tunnel widths. The disparity between trapping (ns - μs) and detrapping (ns - sec) times in the delayed luminescence data may reflect the importance of such dynamical fluctuations, however. It is interesting to note that differences can be observed between the delayed luminescence decay dynamics of different individual nanocrystals,[4] suggesting the existence of static heterogeneity among individual nanocrystals, and also that multiple distinct trap configurations may be sampled during repetitive photoexcitation of the same single nanocrystal. Our model is consistent with these observations. Overall, the evidence in support of a direct mechanistic link between delayed luminescence and luminescence blinking in colloidal semiconductor nanocrystals appears persuasive.

Blinking and delayed luminescence measurements also exhibit interesting contrasts. To assemble an adequate data set for analysis of blinking dynamics, measurements are typically performed for long times on individual NCs, and data from multiple NCs are sometimes then collected together into a single data set that effectively reconstructs the behavior of the NC ensemble. Analogous to the advantages of applying photon-correlation methods at the ensemble level,[32] the delayed luminescence experiment is performed directly on the NC ensemble, and reflects the same (or an even broader) sampling of events without selection bias. Delayed luminescence measurements can be performed on free-standing colloidal NCs, eliminating the effects of NC interactions with substrates or host polymers, which may lead to potential intensity-modification or sample-orientation effects, or even to background luminescence artifacts.[33] On the other hand, delayed luminescence selectively probes carrier detrapping that results in re-formation of the emissive excited state, whereas blinking "off" statistics reflect all detrapping channels that regenerate the NC in its neutral ground state. Finally, ensemble delayed luminescence measurements allow data collection at much lower excitation rates than are

typically used in blinking measurements, enabling traversal from a high-power regime in which the phenomenon is excitation-power independent (as found in blinking "off"-state dynamics[8]) to a low-power regime in which it becomes power dependent.[6] Overall, delayed luminescence measurements thus offer a highly flexible experimental approach to exploring the underlying microscopic processes involved in metastable trapping and detrapping, complementing existing blinking techniques.

Conclusion

Surprisingly similar delayed luminescence dynamics are observed across a variety of colloidal semiconductor NC materials. CdSe, Cu^+:CdSe and $CuInS_2$ NCs all show distinctly non-power-law decay dynamics when measured over 8 decades in time, and these dynamics are independent of temperature from 20 K until at least 160 K, where thermally activated nonradiative decay begins to appear. A model is presented that reproduces the key observations in the delayed luminescence decay and its temperature dependence. This model invokes detrapping *via* tunneling from a nearly degenerate charge-separated metastable state as the rate-determining process in delayed luminescence, and reproduces the data well using a log-normal distribution of tunneling rates, such as obtained from a Gaussian distribution of tunnel widths. Several of the observations made in these delayed luminescence measurements are reminiscent of analogous observations from photoluminescence blinking measurements, and specific relationships between delayed luminescence and blinking are discussed. Delayed luminescence measurements are proposed as a flexible and complementary approach to blinking measurements for understanding the microscopic processes responsible for both phenomena.

Author Information

Corresponding Author
*E-mail: gamelin@chem.washington.edu, Ph (206) 685-0901

[§]Author Present Address
Department of Chemistry, University of Rochester, Rochester, NY 14627, USA

Notes
The authors declare no competing financial interest.

Acknowledgments. Financial support from the National Science Foundation (CHE-1404674 to

P.J.R. and DMR-1505901 to D.R.G.) is gratefully acknowledged. K.E.K. thanks the Department of Energy for support through an Energy Efficiency and Renewable Energy (EERE) postdoctoral research award. A. M. acknowledges the support of an Early Postdoc Mobility Fellowship from the Swiss National Science Foundation. We thank Mr. Luming Yang for synthesis of a Cu^{+}:CdSe sample used in these studies. The authors would like to thank Mr. Michael De Siena and Dr. Sidney Creutz for collecting TEM data. Part of this work was conducted at the Molecular Analysis Facility, which is supported in part by funds from the Molecular Engineering & Sciences Institute, the Clean Energy Institute, the National Science Foundation and the National Institutes of Health.

Supporting Information Available: Additional sample characterization, spectroscopic data, and modeling parameters. This material is available free of charge *via* the Internet at http://pubs.acs.org.

References

(1) Sher, P. H.; Smith, J. M.; Dalgarno, P. A.; Warburton, R. J.; Chen, X.; Dobson, P. J.; Daniels, S. M.; Pickett, N. L.; O'Brien, P., Power Law Carrier Dynamics in Semiconductor Nanocrystals at Nanosecond Timescales. *Appl. Phys. Lett.* **2008,** *92*, 101111.

(2) Jones, M.; Lo, S. S.; Scholes, G. D., Quantitative Modeling of the Role of Surface Traps in CdSe/CdS/ZnS Nanocrystal Photoluminescence Decay Dynamics. *Proc. Natl. Acad. Sci. USA* **2009,** *106*, 3011-3016.

(3) Whitham, P. J.; Knowles, K. E.; Reid, P. J.; Gamelin, D. R., Photoluminescence Blinking and Reversible Electron Trapping in Copper-Doped CdSe Nanocrystals. *Nano Lett.* **2015,** *15*, 4045-4051.

(4) Rabouw, F. T.; Kamp, M.; van Dijk-Moes, R. J.; Gamelin, D. R.; Koenderink, A. F.; Meijerink, A.; Vanmaekelbergh, D., Delayed Exciton Emission and Its Relation to Blinking in CdSe Quantum Dots. *Nano Lett.* **2015,** *15*, 7718-7725.

(5) Rabouw, F. T.; van der Bok, J. C.; Spinicelli, P.; Mahler, B.; Nasilowski, M.; Pedetti, S.; Dubertret, B.; Vanmaekelbergh, D., Temporary Charge Carrier Separation Dominates the Photoluminescence Decay Dynamics of Colloidal CdSe Nanoplatelets. *Nano Lett.* **2016,** *16*, 2047-2053.

(6) Whitham, P. J.; Marchioro, A.; Knowles, K. E.; Kilburn, T. B.; Reid, P. J.; Gamelin, D. R., Single-Particle Photoluminescence Spectra, Blinking, and Delayed Luminescence of Colloidal $CuInS_2$ Nanocrystals. *J. Phys. Chem. C* **2016,** *120*, 17136-17142.

(7) Tachiya, M.; Seki, K., Unified Explanation of the Fluorescence Decay and Blinking Characteristics of Semiconductor Nanocrystals. *Appl. Phys. Lett.* **2009,** *94*, 081104.

(8) Kuno, M.; Fromm, D. P.; Hamann, H. F.; Gallagher, A.; Nesbitt, D. J., "On"/"Off" Fluorescence Intermittency of Single Semiconductor Quantum Dots. *J. Chem. Phys.* **2001,** *115*, 1028-1040.

(9) Kuno, M.; Fromm, D. P.; Hamann, H. F.; Gallagher, A.; Nesbitt, D. J., Nonexponential "Blinking" Kinetics of Single CdSe Quantum Dots: A Universal Power Law Behavior. *J. Chem. Phys.* **2000,** *112*, 3117-3120.

(10) Verberk, R.; van Oijen, A. M.; Orrit, M., Simple Model for the Power-Law Blinking of Single Semiconductor Nanocrystals. *Phys. Rev. B* **2002,** *66*, 233202.

(11) Kuno, M.; Fromm, D. P.; Johnson, S. T.; Gallagher, A.; Nesbitt, D. J., Modeling Distributed Kinetics in Isolated Semiconductor Quantum Dots. *Phys. Rev. B* **2003,** *67*, 125304.

(12) Tang, J.; Marcus, R. A., Diffusion-Controlled Electron Transfer Processes and Power-Law Statistics of Fluorescence Intermittency of Nanoparticles. *Phys. Rev. Lett.* **2005,** *95*, 107401.
(13) Frantsuzov, P. A.; Marcus, R. A., Explanation of Quantum Dot Blinking without the Long-Lived Trap Hypothesis. *Phys. Rev. B* **2005,** *72*, 155321.
(14) Pelton, M.; Smith, G.; Scherer, N. F.; Marcus, R. A., Evidence for a Diffusion-Controlled Mechanism for Fluorescence Blinking of Colloidal Quantum Dots. *Proc. Natl. Acad. Sci. USA* **2007,** *104*, 14249-14254.
(15) Frantsuzov, P. A.; Volkan-Kacso, S.; Janko, B., Model of Fluorescence Intermittency of Single Colloidal Semiconductor Quantum Dots Using Multiple Recombination Centers. *Phys. Rev. Lett.* **2009,** *103*, 207402.
(16) Galland, C.; Ghosh, Y.; Steinbruck, A.; Sykora, M.; Hollingsworth, J. A.; Klimov, V. I.; Htoon, H., Two Types of Luminescence Blinking Revealed by Spectroelectrochemistry of Single Quantum Dots. *Nature* **2011,** *479*, 203-207.
(17) Qin, W.; Guyot-Sionnest, P., Evidence for the Role of Holes in Blinking: Negative and Oxidized CdSe/CdS Dots. *ACS Nano* **2012,** *6*, 9125-9132.
(18) Li, L.; Pandey, A.; Werder, D. J.; Khanal, B. P.; Pietryga, J. M.; Klimov, V. I., Efficient Synthesis of Highly Luminescent Copper Indium Sulfide-Based Core/Shell Nanocrystals with Surprisingly Long-Lived Emission. *J. Am. Chem. Soc.* **2011,** *133*, 1176-1179.
(19) Chen, O.; Chen, X.; Yang, Y.; Lynch, J.; Wu, H.; Zhuang, J.; Cao, Y. C., Synthesis of Metal-Selenide Nanocrystals Using Selenium Dioxide as the Selenium Precursor. *Angew. Chem. Int. Ed.* **2008,** *47*, 8638-8641.
(20) Piepho, S. B.; Schatz, P. N., *Group Theory in Spectroscopy with Applications to Magnetic Circular Dichroism*. John Wiley & Sons Inc: 1983.
(21) Knowles, K. E.; Hartstein, K. H.; Kilburn, T. B.; Marchioro, A.; Nelson, H. D.; Whitham, P. J.; Gamelin, D. R., Luminescent Colloidal Semiconductor Nanocrystals Containing Copper: Synthesis, Photophysics, and Applications. *Chem. Rev.* **2016,** *116*, 10820–10851.
(22) Zhong, H.; Zhou, Y.; Ye, M.; He, Y.; Ye, J.; He, C.; Yang, C.; Li, Y., Controlled Synthesis and Optical Properties of Colloidal Ternary Chalcogenide $CuInS_2$ Nanocrystals. *Chem. Mater.* **2008,** *20*, 6434-6443.
(23) Tran, T. K. C.; Le, Q. P.; Nguyen, Q. L.; Li, L.; Reiss, P., Time-Resolved Photoluminescence Study of $CuInS_2$/ZnS Nanocrystals. *Adv. Nat. Sci.: Nanosci. Nanotechnol.* **2010,** *1*, 025007.
(24) Sun, J.; Ikezawa, M.; Wang, X.; Jing, P.; Li, H.; Zhao, J.; Masumoto, Y., Photocarrier Recombination Dynamics in Ternary Chalcogenide $CuInS_2$ Quantum Dots. *Phys. Chem. Chem. Phys.* **2015,** *17*, 11981-11989.
(25) Knowles, K. E.; Nelson, H. D.; Kilburn, T. B.; Gamelin, D. R., Singlet-Triplet Splittings in the Luminescent Excited States of Colloidal Cu^+:CdSe, Cu^+:InP, and $CuInS_2$ Nanocrystals: Charge-Transfer Configurations and Self-Trapped Excitons. *J. Am. Chem. Soc.* **2015,** *137*, 13138-13147.
(26) Shimizu, K. T.; Neuhauser, R. G.; Leatherdale, C. A.; Empedocles, S. A.; Woo, W. K.; Bawendi, M. G., Blinking Statistics in Single Semiconductor Nanocrystal Quantum Dots. *Phys. Rev. B* **2001,** *63*, 205316.
(27) Riley, E. A.; Hess, C. M.; Whitham, P. J.; Reid, P. J., Beyond Power Laws: A New Approach for Analyzing Single Molecule Photoluminescence Intermittency. *J. Chem. Phys.* **2012,** *136*, 184508.

(28) Mitsui, M.; Unno, A.; Azechi, S., Understanding Photoinduced Charge Transfer Dynamics of Single Perylenediimide Dyes in a Polymer Matrix by Bin-Time Dependence of Their Fluorescence Blinking Statistics. *J. Phys. Chem. C* **2016,** *120*, 15070-15081.
(29) Riley, E. A.; Hess, C. M.; Pioquinto, J. R.; Kaminsky, W.; Kahr, B.; Reid, P. J., Proton Transfer and Photoluminescence Intermittency of Single Emitters in Dyed Crystals. *J. Phys. Chem. B* **2013,** *117*, 4313-4324.
(30) Nirmal, M.; Dabbousi, B. O.; Bawendi, M. G.; Macklin, J. J.; Trautman, J. K.; Harris, T. D.; Brus, L. E., Fluorescence Intermittency in Single Cadmium Selenide Nanocrystals. *Nature* **1996,** *383*, 802-804.
(31) Banin, U.; Bruchez, M.; Alivisatos, A. P.; Ha, T.; Weiss, S.; Chemla, D. S., Evidence for a Thermal Contribution to Emission Intermittency in Single CdSe/CdS Core/Shell Nanocrystals. *J. Chem. Phys.* **1999,** *110*, 1195-1201.
(32) Beyler, A. P.; Bischof, T. S.; Cui, J.; Coropceanu, I.; Harris, D. K.; Bawendi, M. G., Sample-Averaged Biexciton Quantum Yield Measured by Solution-Phase Photon Correlation. *Nano Lett.* **2014,** *14*, 6792-6798.
(33) Rabouw, F. T.; Cogan, N. M. B.; Berends, A. C.; van der Stam, W.; Vanmaekelbergh, D.; Koenderink, A. F.; Krauss, T. D.; de Mello Donega, C., Non-Blinking Single-Photon Emitters in Silica. *Sci. Rep.* **2016,** *6*, 21187.

TOC Graphic:

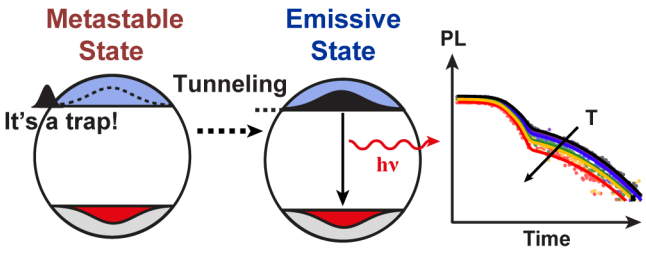
Metastable State
Emissive State
PL
Tunneling
It's a trap!
hν
T
Time